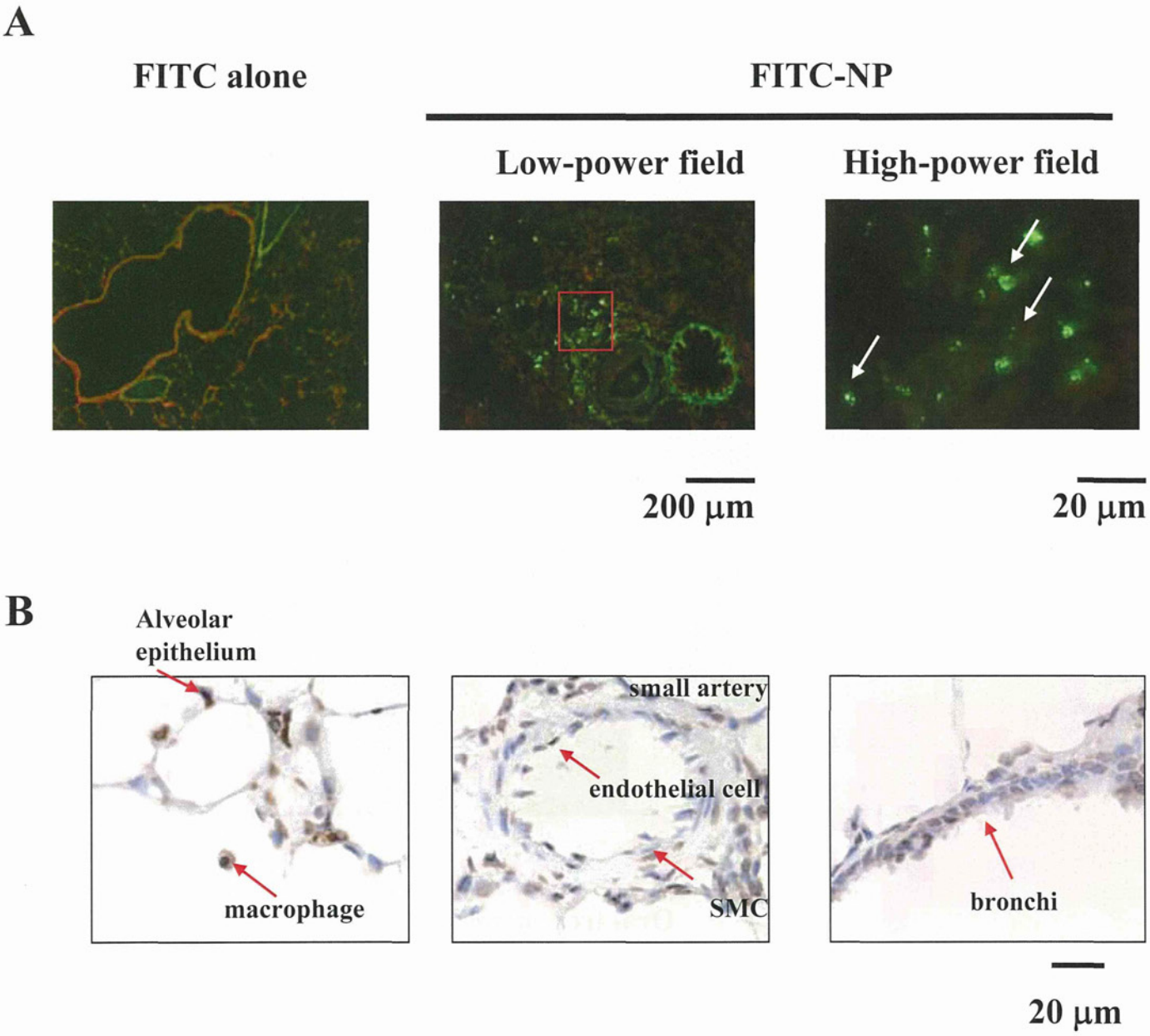

Figure S1. Localization of FITC alone and FITC-NP post-instillation in the rat lung. A, Fluorescent micrographs of cross-sections from lung instillated with FITC alone and FITC-labeled NP on day 3 post-instillation. Nuclei were counterstained with propidium iodide (red). Scale bars: 200 μm and 20 μm.
B, Micrographs of cross-sections stained immunohistochemically against FITC from lung instillated intratracheally with FITC-NP on days 14 post-instillation.

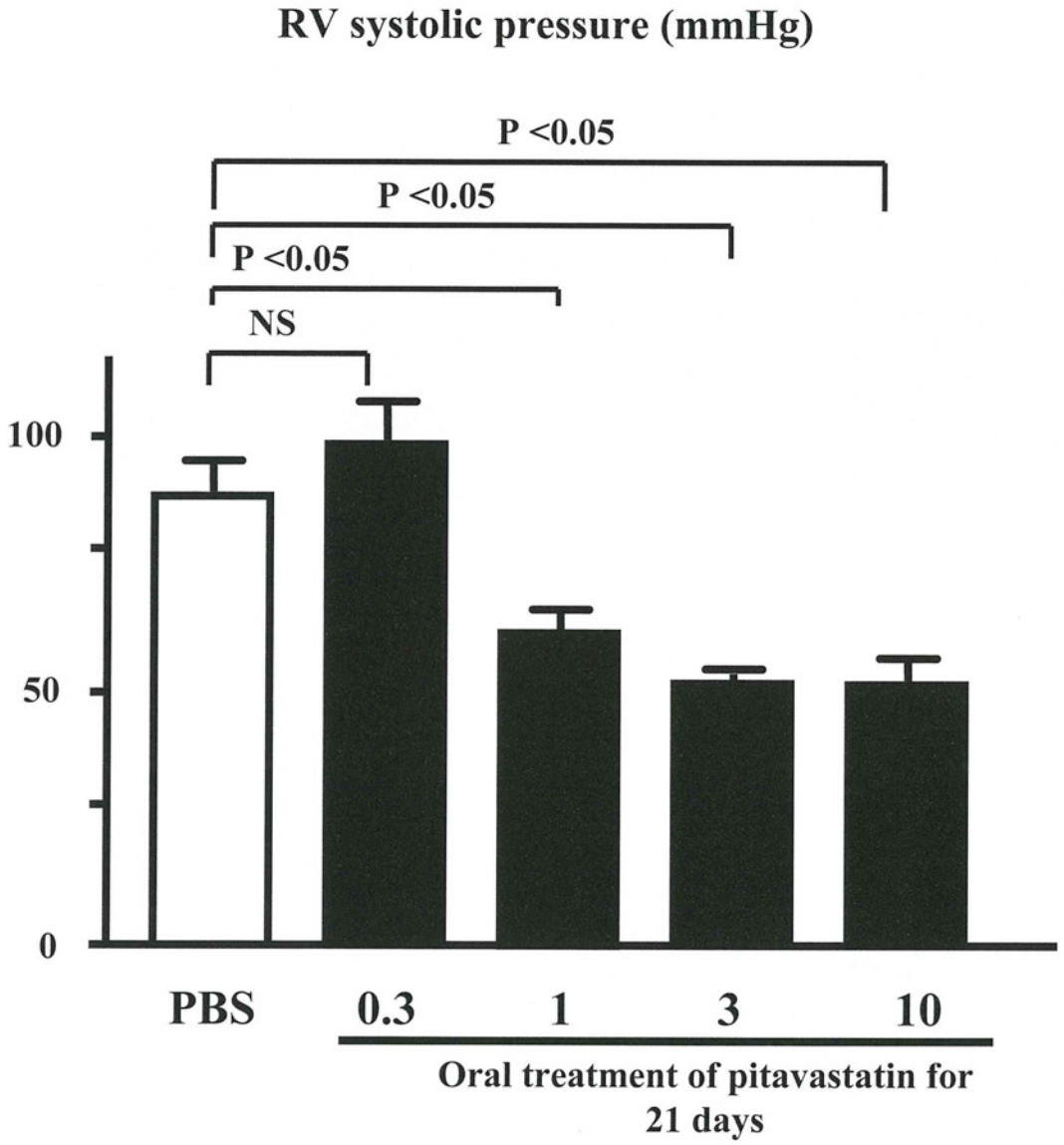

Figure S2. Effects of oral treatment of pitavastatin on right ventricular (RV) systolic pressure 3 weeks after MCT injection. Data are mean ± SEM ($n = 6$ each).

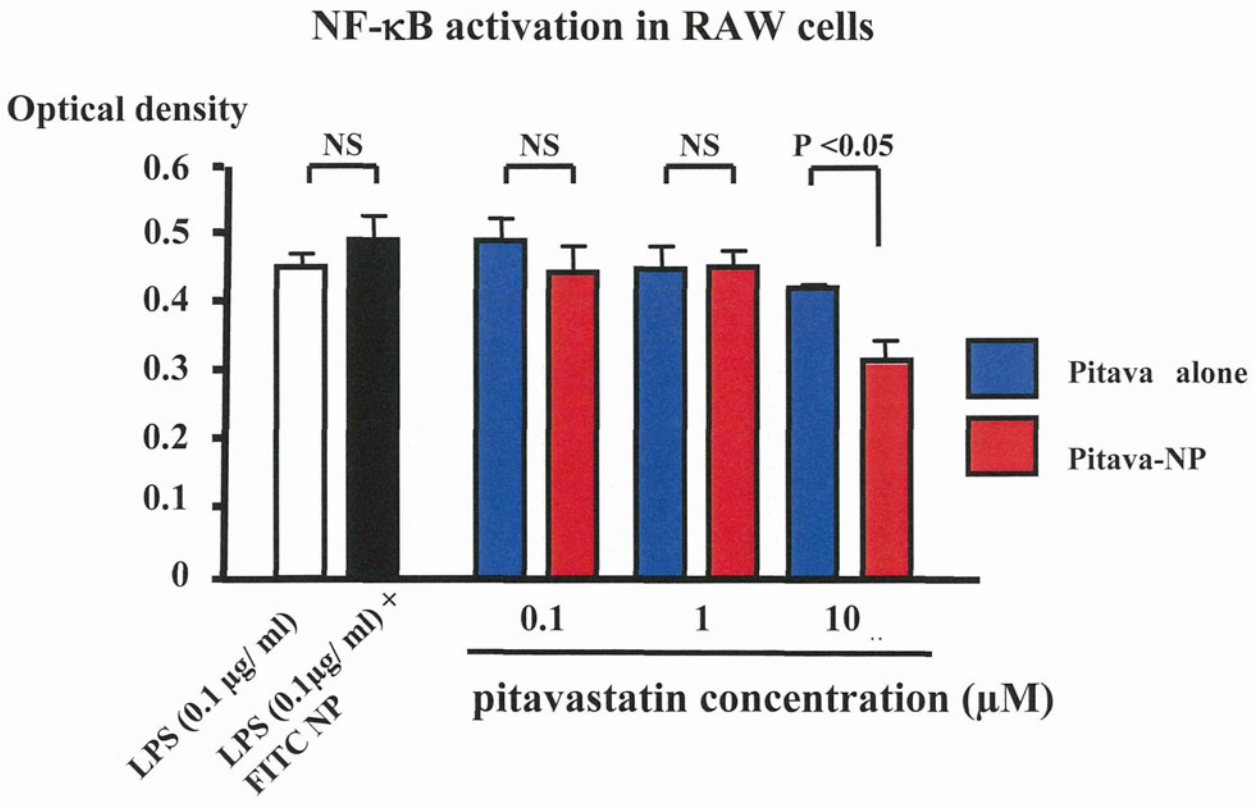

Figure S3 Effect of pitavastatin-NP on NF-κB activation of monocyte cell line (RAW cells)
Effects of pitavastatin-NP on LPS-stimulated activation of NF−κB (ELISA-based DNA binding assay against NF-kB p65 subunit: arbitrary unit). Data are mean ± SEM (n= 6 each).

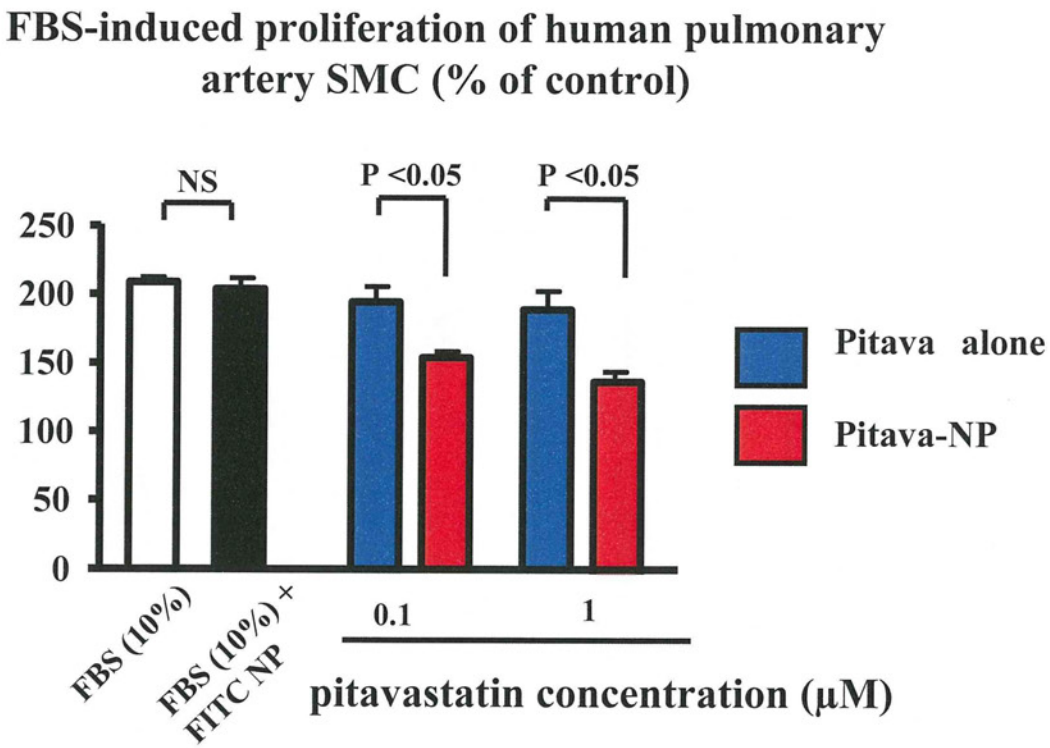

Figure S4. Effects of pitavastatin-NP versus pitavastatin on FBS-induced proliferation of human PASMCs (cell count per well). Data are mean ± SEM (n = 6 each).

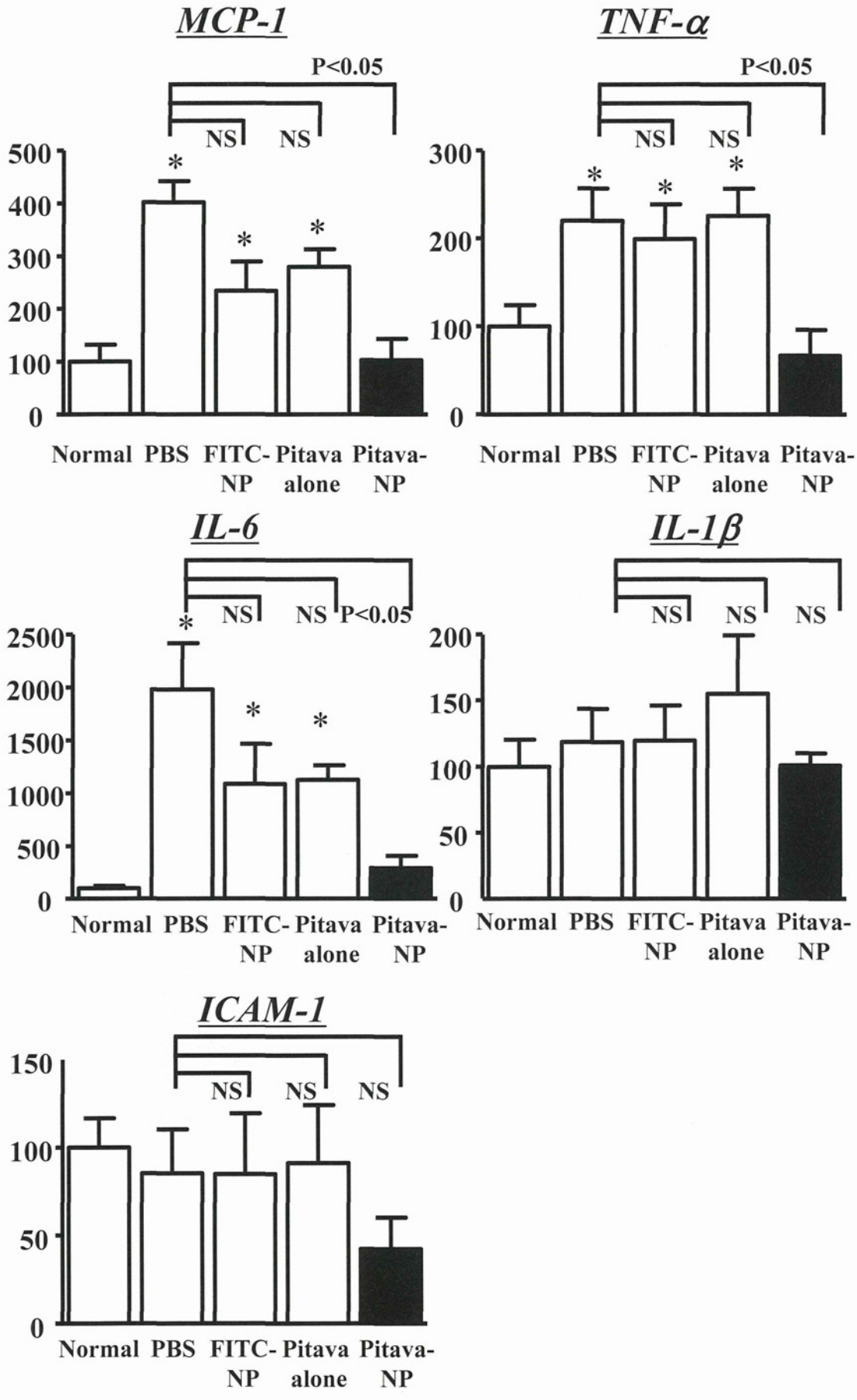

Figure S5. Effects of pitavastatin-NP on mRNA levels of various inflammatory and proliferative factors 21 days after MCT injection (n = 6 each). *$P < 0.05$ versus Normal. Data are mean ±SEM. NS; Not Significant.

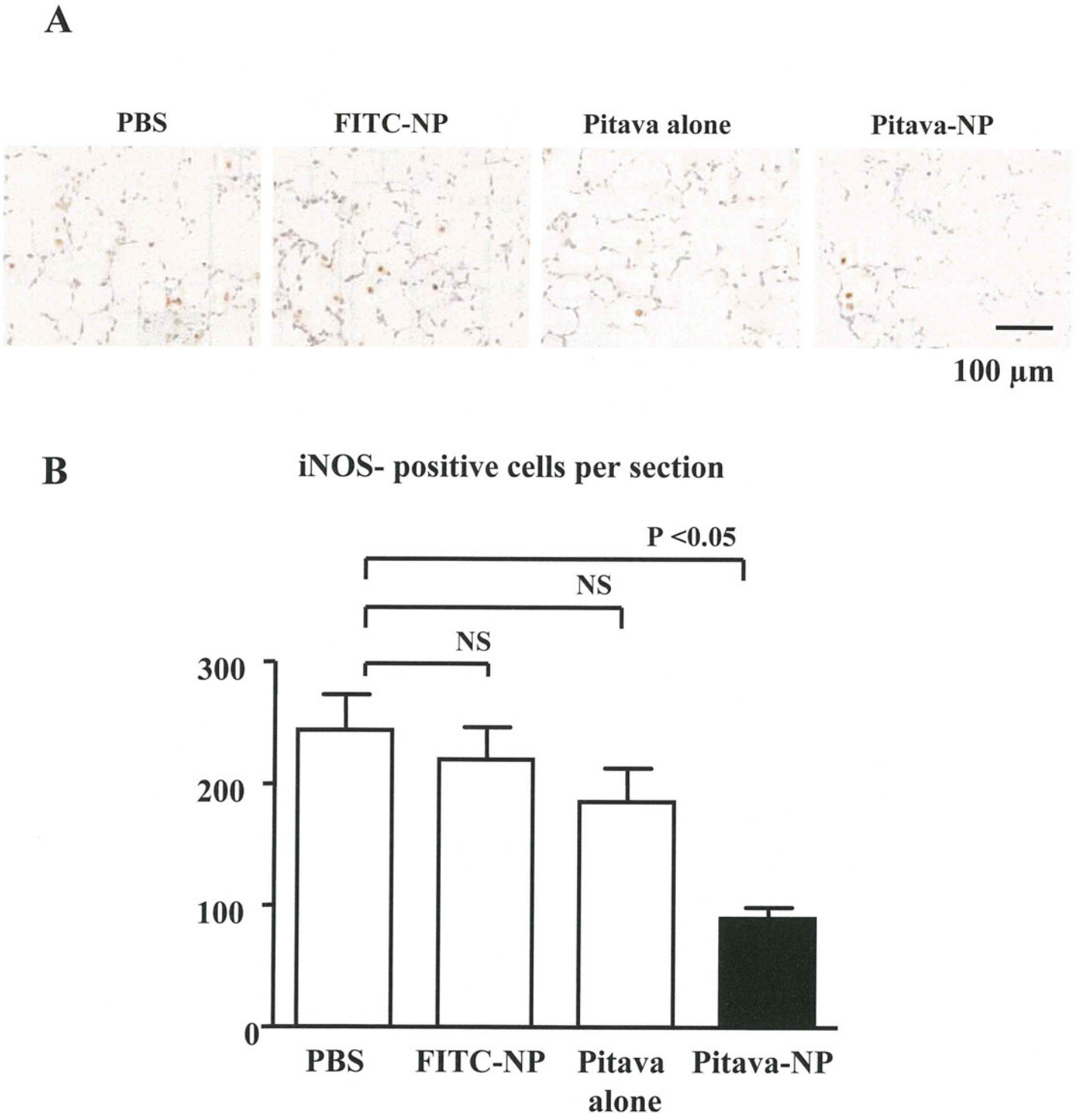

Figure S6. Effects of pitavastatin-NP on iNOS protein expression
A, Representative micrographs of lung tissues stained immunohistochemically for iNOS.
B, Effects of pitavastatin-NP on infiltration of iNOS-positive cells 21 days after MCT injection. Data are mean ±SEM (n = 6 each).

Circulation Journal
Official Journal of the Japanese Circulation Society
http://www.j-circ.or.jp

ORIGINAL ARTICLE
Hypertension and Circulatory Control

Medetomidine, an α_2-Adrenergic Agonist, Activates Cardiac Vagal Nerve Through Modulation of Baroreflex Control

Shuji Shimizu, MD, PhD; Tsuyoshi Akiyama, MD, PhD; Toru Kawada, MD, PhD; Yusuke Sata, MD; Masaki Mizuno, PhD; Atsunori Kamiya, MD, PhD; Toshiaki Shishido, MD, PhD; Masashi Inagaki, MD; Mikiyasu Shirai, MD, PhD; Shunji Sano, MD, PhD; Masaru Sugimachi, MD, PhD

Background: Although α_2-adrenergic agonists have been reported to induce a vagal-dominant condition through suppression of sympathetic nerve activity, there is little direct evidence that they directly increase cardiac vagal nerve activity. Using a cardiac microdialysis technique, we investigated the effects of medetomidine, an α_2-adrenergic agonist, on norepinephrine (NE) and acetylcholine (ACh) release from cardiac nerve endings.

Methods and Results: A microdialysis probe was implanted into the right atrial wall near the sinoatrial node in anesthetized rabbits and perfused with Ringer's solution containing eserine. Dialysate NE and ACh concentrations were measured using high-performance liquid chromatography. Both 10 and 100 μg/kg of intravenous medetomidine significantly decreased mean blood pressure (BP) and the dialysate NE concentration, but only 100 μg/kg of medetomidine enhanced ACh release. Combined administration of medetomidine and phenylephrine maintained mean BP at baseline level, and augmented the medetomidine-induced ACh release. When we varied the mean BP using intravenous administration of phenylephrine, treatment with medetomidine significantly steepened the slope of the regression line between mean BP and log ACh concentration.

Conclusions: Medetomidine increased ACh release from cardiac vagal nerve endings and augmented baroreflex control of vagal nerve activity. (*Circ J* 2012; **76:** 152–159)

Key Words: Acetylcholine; Norepinephrine; Sinoatrial node; Sympathetic nervous system; Vagus nerve

The selective α_2-adrenergic agonist, dexmedetomidine, is widely used for sedation in intensive care units because it has a less respiratory depressive effect.[1] In addition, several benefits of dexmedetomidine that favor its use in intensive care have been reported, such as reduced opioid dosage requirement. In animal studies, Hayashi et al reported that dexmedetomidine prevented epinephrine-induced arrhythmias in halothane-anesthetized dogs.[2] This antiarrhythmic effect of α_2-adrenergic agonists may be partly ascribed to vagal activation.[3] It has already been reported that central sympathetic inhibition by an α_2-adrenergic agonist, guanfacine, augmented the sleep-related ultradian rhythm of parasympathetic tone in patients with chronic heart failure.[4] Although α_2-adrenergic agonists are widely recognized as inducing a vagal-dominant condition through the suppression of sympathetic nerve, there is little direct evidence that they directly increase cardiac vagal nerve activity, because such activity has been assessed only by indirect methods, such as heart rate variability, in most studies.[5]

Vanoli et al[6] reported that vagal stimulation after an acute ischemic episode effectively prevented ventricular fibrillation in dogs. Their group also indicated that the dogs that developed ventricular fibrillation during the acute ischemic episode had a significantly lower baroreflex-mediated heart rate response,[7] suggesting the importance of the baroreflex in controlling vagal function. If an α_2-adrenergic agonist is able to activate the cardiac vagal nerve directly or via modulation of the baroreflex function, it will provide a new therapeutic option for life-threatening arrhythmias after myocardial ischemia.

Medetomidine is a racemic mixture of 2 stereoisomers, dexmedetomidine and levomedetomidine. However, because it has already been reported that levomedetomidine has no effect on cardiovascular parameters and causes no apparent sedation or analgesia,[8] the pharmacokinetics of dexmedetomidine and racemic medetomidine are almost similar. We hypothesized that medetomidine can activate the cardiac vagal nerve

Received June 1, 2011; revised manuscript received September 6, 2011; accepted September 14, 2011; released online October 29, 2011
Time for primary review: 25 days

Department of Cardiovascular Dynamics (S. Shimizu, T.K., Y.S., M.M., A.K., T.S., M.I., M. Sugimachi), Department of Cardiac Physiology (T.A., M. Shirai), National Cerebral and Cardiovascular Center Research Institute, Suita; and Department of Cardiovascular Surgery, Okayama University Graduate School of Medicine, Dentistry and Pharmaceutical Sciences, Okayama (S. Sano), Japan
Mailing address: Shuji Shimizu, MD, PhD, Department of Cardiovascular Dynamics, National Cerebral and Cardiovascular Center Research Institute, 5-7-1 Fujishiro-dai, Suita 565-8565, Japan. E-mail: shujismz@ri.ncvc.go.jp

ISSN-1346-9843 doi:10.1253/circj.CJ-11-0574

through a central action and improve the baroreflex control of vagal nerve activity. We have established a cardiac microdialysis technique for separate monitoring of neuronal norepinephrine (NE) and acetylcholine (ACh) release to the rabbit sinoatrial (SA) node in vivo.[9–11] Using this microdialysis technique, we investigated the effects of medetomidine on cardiac autonomic nerve activities innervating the SA node.

Methods

Surgical Preparation

Animal care was provided in accordance with the "Guiding principles for the care and use of animals in the field of physiological sciences" published by the Physiological Society of Japan. All protocols were approved by the Animal Subject Committee of the National Cerebral and Cardiovascular Center.

In this study, 31 Japanese white rabbits weighing 2.3–3.0 kg were used. Anesthesia was initiated by an intravenous injection of pentobarbital sodium (50 mg/kg) via the marginal ear vein, and then maintained at an appropriate level by continuous intravenous infusion of α-chloralose and urethane (16 mg·kg^{-1}·h^{-1} and 100 mg·kg^{-1}·h^{-1}) through a catheter inserted into the femoral vein. The animals were intubated and ventilated mechanically with room air mixed with oxygen. Respiratory rate and tidal volume were set at 30 cycles/min and 15 ml/kg, respectively. Systemic arterial pressure was monitored by a catheter inserted into the femoral artery. Esophageal temperature, which was measured by a thermometer (CTM-303, Terumo, Japan), was maintained between 38°C and 39°C using a heating pad.

With the animal in lateral position, a right lateral thoracotomy was performed and the right 3rd to 5th ribs were partially resected to expose the heart. After incising the pericardium, a dialysis probe was implanted as described below. Three stainless steel electrodes were attached around the thoracotomy incision for recording body surface electrocardiogram (ECG). The heart rate was determined from the ECG using a cardiotachometer. Heparin sodium (100 IU/kg) was administered intravenously to prevent blood coagulation. At the end of the experiment, the animal was killed humanely by injecting an overdose of pentobarbital sodium. In the postmortem examination, the right atrial wall was resected en bloc with the dialysis probe. The inside of the atrial wall was observed macroscopically to confirm that the dialysis membrane was not exposed to the right atrial lumen.

Dialysis Technique

The materials and properties of the dialysis probe have been described previously.[9–12] A dialysis fiber of semipermeable membrane (length 4 mm, outer diameter 310 μm, inner diameter 200 μm, PAN-1200, molecular weight cutoff 50,000; Asahi Chemical, Tokyo, Japan) was attached at both ends to polyethylene tubes (length 25 cm, outer diameter 500 μm, inner diameter 200 μm). A fine guiding needle (length 30 mm, outer diameter 510 μm, inner diameter 250 μm) with a stainless steel rod (length 5 mm, outer diameter 250 μm) was used for the implantation of the dialysis probe. A dialysis probe was implanted into the right atrial myocardium near the junction of the superior vena cava and the right atrium. After implantation, the dialysis probe was perfused with Ringer's solution (in mmol/L: NaCl 147, KCl 4, $CaCl_2$ 3) containing a cholinesterase inhibitor eserine (100 μmol/L), at a speed of 2 μl/min using a microinjection pump (CMA/102, Carnegie Medicin, Sweden). Experimental protocols were started 120 min after implantation of the dialysis probe. The dead space between the dialysis membrane and the sample tube was taken into account at the beginning of each dialysate sampling. In protocols 1 and 2 as described below, 8 μl of phosphate buffer (pH 3.5) was added to each sample tube before dialysate sampling, and each dialysate sampling period was set at 20 min (1 sample volume=40 μl). Half of the dialysate sample was used for ACh and the other half for NE measurements. In protocol 3, 2 μl of phosphate buffer was added to each sample tube before dialysate sampling, and each dialysate sampling period was set at 5 min (1 sample volume=10 μl). In protocol 4, 4 μl of phosphate buffer was added to each sample tube before dialysate sampling, and each dialysate sampling period was set at 10 min (1 sample volume=20 μl). Dialysate NE and ACh concentrations were analyzed separately by high-performance liquid chromatography as described previously.[12,13]

Experimental Protocols

Protocol 1 (n=7) Baseline dialysate was sampled before the injection of medetomidine. Thereafter, a low dose (10 μg/kg) of medetomidine was injected intravenously via the femoral vein. After allowing 20 min for hemodynamic stabilization, dialysate was sampled for 20 min (40 μl). When the hemodynamics had recovered to the baseline level, a high dose (100 μg/kg) of medetomidine was injected intravenously and another 20-min dialysate sample was collected after hemodynamic stabilization. Finally, the vagal nerves were sectioned bilaterally at the neck and a dialysate sample was collected immediately after vagotomy. In 4 rabbits, an α_2-adrenergic antagonist, atipamezole (2.5 mg/kg), was intravenously administered before euthanasia and hemodynamic responses were recorded.

Protocol 2 (n=7) To prevent possible interference of medetomidine-induced hypotension with vagal nerve activity, intravenous infusion of an α_1-adrenergic agonist, phenylephrine, was started simultaneous to intravenous injection of medetomidine. Baseline dialysate sample was collected for 20 min before medetomidine injection. Simultaneous to intravenous injection of high-dose (100 μg/kg) medetomidine, intravenous infusion of phenylephrine was started (6.6±1.2 μg·kg^{-1}·min^{-1}) to maintain the mean blood pressure (BP) at baseline level. After hemodynamic stabilization, dialysate was sampled for 20 min. Finally, dialysate was again sampled immediately after bilateral cervical vagotomy.

Protocol 3 To investigate the effect of medetomidine on baroreflex-induced vagal ACh release, we varied the mean BP by changing the dose of intravenous phenylephrine in both the control (n=5) and medetomidine-treated (n=7) groups. In the control group, Ringer's solution was infused intravenously at 1.0 ml·kg^{-1}·h^{-1} throughout the experiment. In the medetomidine-treated group, medetomidine was initially injected intravenously at a dose of 60 μg/kg, and thereafter continuously infused at a dose of 60 μg·kg^{-1}·h^{-1} or a rate of 1.0 ml·kg^{-1}·h^{-1}. After baseline dialysate sampling, mean BP was increased in a stepwise manner by altering the dose of intravenous phenylephrine (maximal dose: 32.2±5.5 μg·kg^{-1}·min^{-1} in the control group and 18.6±2.1 μg·kg^{-1}·min^{-1} in the medetomidine-treated group). Dialysate samples were collected for 5 min at 4–7 different mean BP levels. Relations of log ACh concentrations vs. mean BP were plotted and regression lines for each animal were calculated.

Protocol 4 (n=5) We investigated the peripheral effects of medetomidine on heart rate and dialysate ACh concentration under electrical stimulation of the right cervical vagal nerve. Bilateral vagal nerves were exposed through a midline cervical incision and sectioned at the neck. A pair of bipolar stainless steel electrodes was attached to the efferent side of the

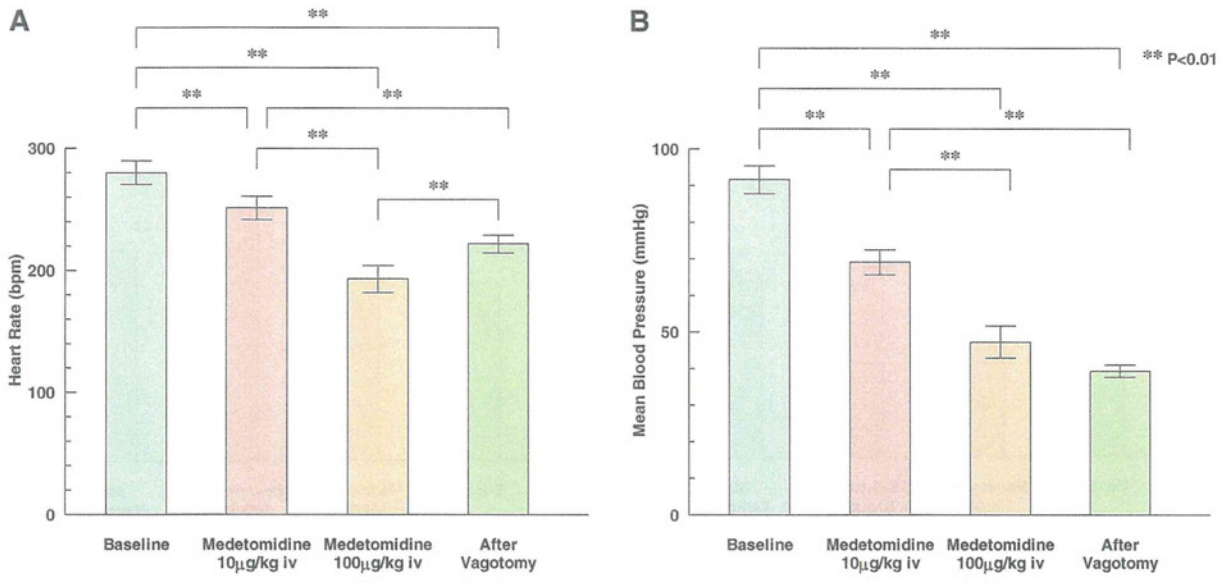

Figure 1. Intravenous administration of low and high doses of medetomidine decreased heart rate (**A**) and mean blood pressure (**B**). Medetomidine decreased heart rate in a dose-dependent manner. Vagotomy partially restored the decrease in heart rate but had no effect on mean blood pressure under administration of 100 μg/kg of medetomidine. **P<0.01.

right vagal nerve. The nerve and electrode were covered with warmed mineral oil for insulation. After the baseline dialysate sampling, the right efferent vagal nerve was stimulated at the frequency of 20 Hz by a digital stimulator (SEN-7203, Nihon Kohden, Japan). The pulse duration and amplitude of nerve stimulation were set at 1 ms and 10 V. Thereafter, a low dose (10 μg/kg) of medetomidine was injected intravenously via the femoral vein. After hemodynamic stabilization, dialysate was sampled for 10 min under the 20-Hz electrical stimulation of vagal nerve. Finally, a high dose (100 μg/kg) of medetomidine was injected intravenously and another 10-min dialysate sample was collected under the 20-Hz electrical stimulation.

Statistical Analysis

All data are presented as mean±standard error. Heart rate and mean BP were compared by 1-way repeated measures analysis of variance (ANOVA) followed by a Tukey's test.[14] Dialysate NE and ACh concentrations were also compared by 1-way repeated measures ANOVA followed by a Tukey's test. Comparisons of data between protocols 1 and 2 were conducted using unpaired t-test (Student's or Welch's t-test). In protocol 3, the average slopes and intercepts of the regression lines were compared using unpaired t-test. Differences were considered significant at P<0.05.

Results

Protocol 1

Intravenous injection of medetomidine significantly decreased heart rate (Figure 1A) and mean BP (Figure 1B) in a dose-dependent manner (280±10 beats/min and 92±4 mmHg, respectively, at baseline; 251±10 beats/min and 69±3 mmHg at 10 μg/kg; and 193±11 beats/min and 47±4 mmHg at 100 μg/kg, P<0.01 for all comparisons). Vagotomy increased heart rate to 222±7 beats/min but did not affect mean BP (Figures 1A,B).

Low-dose medetomidine significantly decreased dialysate NE concentration (Figure 2A) from 0.72±0.06 to 0.59±0.04 nmol/L (P<0.01) but did not affect dialysate ACh concentration (Figure 2B) compared with baseline. High-dose medetomidine also decreased dialysate NE concentration (to 0.52±0.05 nmol/L) similar to low-dose medetomidine (Figure 2A) and significantly increased dialysate ACh concentration from 7.2±1.3 nmol/L at baseline to 12.1±1.6 nmol/L (P<0.01, Figure 2B). Dialysate NE concentration was not changed by vagotomy, whereas dialysate ACh concentration recovered to the baseline level immediately after vagotomy (Figures 2A,B).

In 4 rabbits treated with atipamezole, heart rate and mean BP recovered to the baseline levels immediately after the injection (276±18 beats/min and 88±6 mmHg, respectively, at baseline; and 280±11 beats/min and 83±6 mmHg after the injection).

Protocol 2

Intravenous injection of high-dose medetomidine combined with phenylephrine decreased heart rate (Figure 3A) and the decrease was significantly greater than that observed in protocol 1 (140±9 vs. 193±11 beats/min, P<0.01), while mean BP was maintained at the same level as baseline (Figure 3B). Medetomidine combined with phenylephrine decreased dialysate NE concentration from 0.85±0.09 at baseline to 0.68±0.10 nmol/L (Figure 4A), and the decrease was not significantly different from that of medetomidine alone (protocol 1). However, medetomidine combined with phenylephrine increased dialysate ACh concentration (Figure 4B) to a significantly and markedly higher level than that observed in protocol 1 (26.8±5.4 vs. 12.1±1.6 nmol/L, P<0.05). Dialysate ACh concentration recovered to the baseline level immediately after vagotomy.

Protocol 3

The change in mean BP by phenylephrine administration affected dialysate ACh concentration only slightly in the control group (Figure 5A), whereas the elevation of mean BP

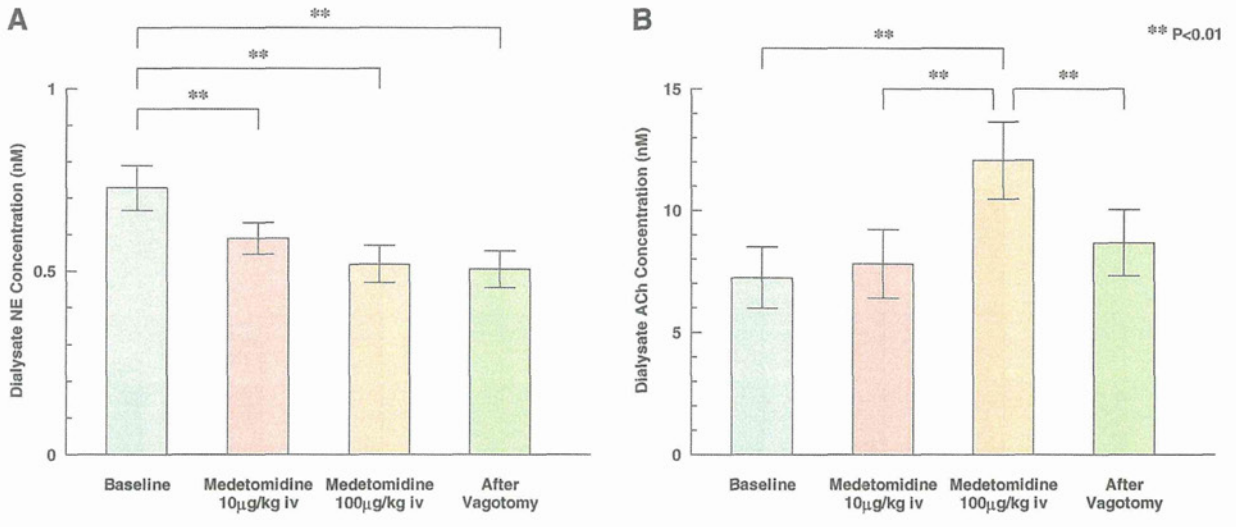

Figure 2. Effects of intravenous administration of low and high doses of medetomidine on dialysate NE (**A**) and ACh concentrations (**B**). Medetomidine at 10 and 100 μg/kg similarly decreased dialysate NE concentration (**A**). Medetomidine at 100 μg/kg significantly increased dialysate ACh concentration, but 10 μg/kg had no effect (**B**). Vagotomy suppressed the increase in dialysate ACh concentration. **P<0.01. ACh, acetylcholine; NE, norepinephrine.

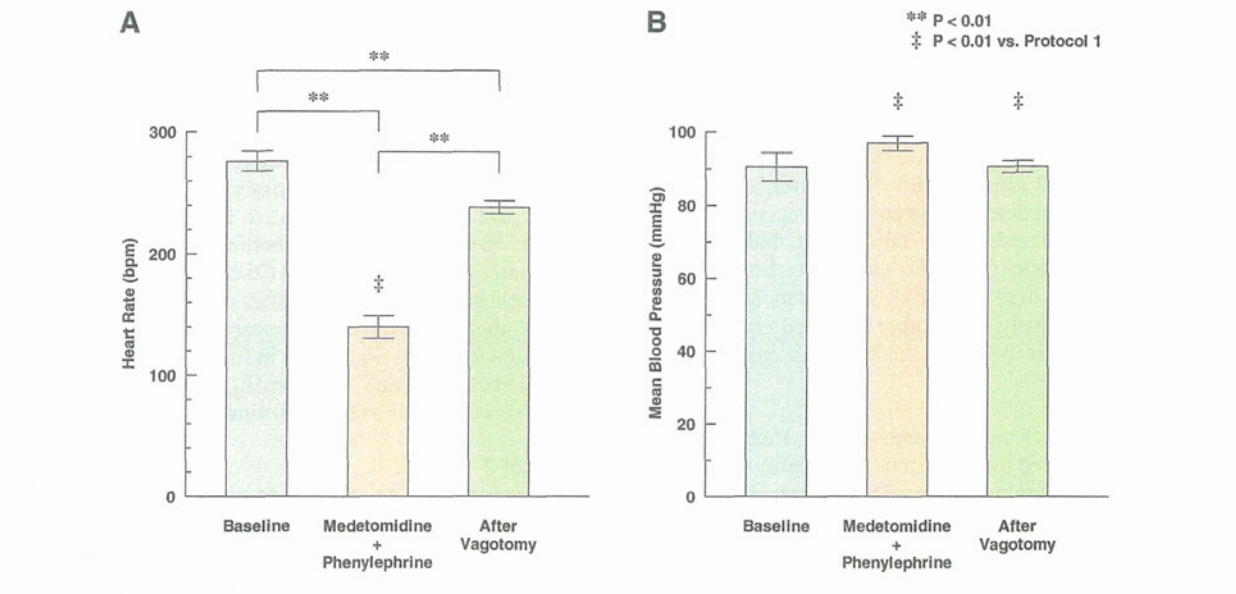

Figure 3. Effects of simultaneous intravenous administration of medetomidine and phenylephrine on heart rate (**A**) and mean blood pressure (**B**). Medetomidine combined with phenylephrine significantly decreased heart rate (**A**), and the decrease was significantly greater compared with medetomidine alone (protocol 1: **Figure 1A**). Medetomidine combined with phenylephrine maintained mean blood pressure (**B**) at the baseline level. Vagotomy partially restored the decrease in heart rate but had no effect on mean blood pressure. **P<0.01; ‡P<0.01 vs. medetomidine alone (protocol 1: **Figure 1A**).

markedly increased dialysate ACh concentration in the medetomidine-treated group (**Figure 5B**). The average slopes of the regression lines between mean BP and log dialysate ACh concentration were 0.0018±0.0004 in the control and 0.0062±0.0006 in the medetomidine-treated group. The slope was significantly steeper in the medetomidine-treated group than that in the control (P<0.01). However, the intercept did not differ significantly between the control (0.59±0.05) and medetomidine-treated (0.68±0.07) groups.

Protocol 4

The 20-Hz electrical stimulation of the right vagal nerve significantly decreased heart rate from 271±11 beats/min at the baseline to 112±6 beats/min and increased dialysate ACh concentration from 7.1±0.9 nmol/L at the baseline to 38.5± 7.2 nmol/L (P<0.01). However, both 10 and 100 μg/kg of me-

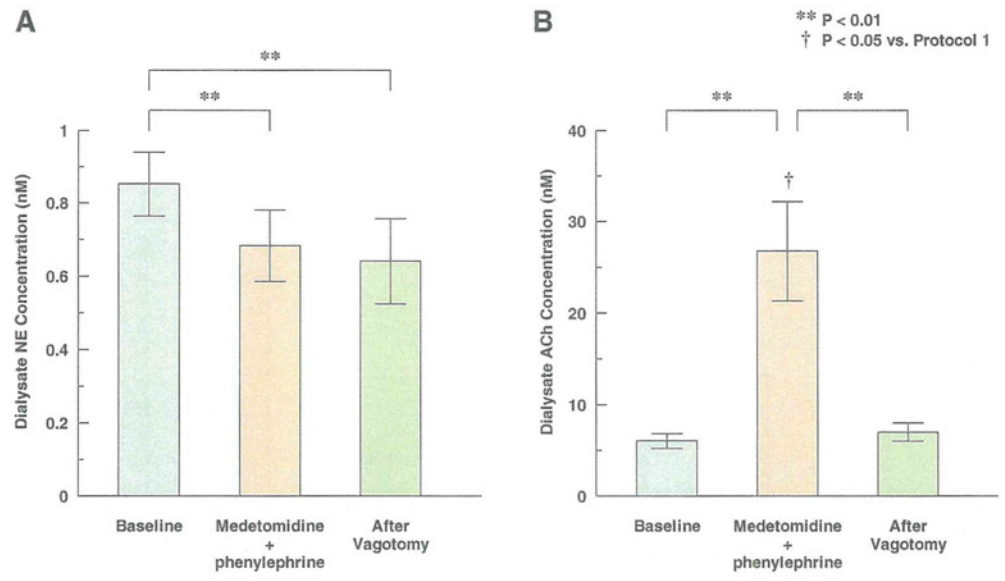

Figure 4. Effects of simultaneous intravenous administration of medetomidine and phenylephrine on dialysate NE (**A**) and ACh concentrations (**B**). Medetomidine combined with phenylephrine decreased dialysate NE concentration (**A**), and the decrease was similar to medetomidine alone (protocol 1: **Figure 2A**). Medetomidine combined with phenylephrine caused a marked increase in dialysate ACh concentration (**B**) and the increase was significantly greater than medetomidine alone (protocol 1: **Figure 2B**). Vagotomy suppressed the increase in dialysate ACh concentration. **P<0.01; †P<0.05 vs. medetomidine alone (protocol 1: **Figure 2B**). ACh, acetylcholine; NE, norepinephrine.

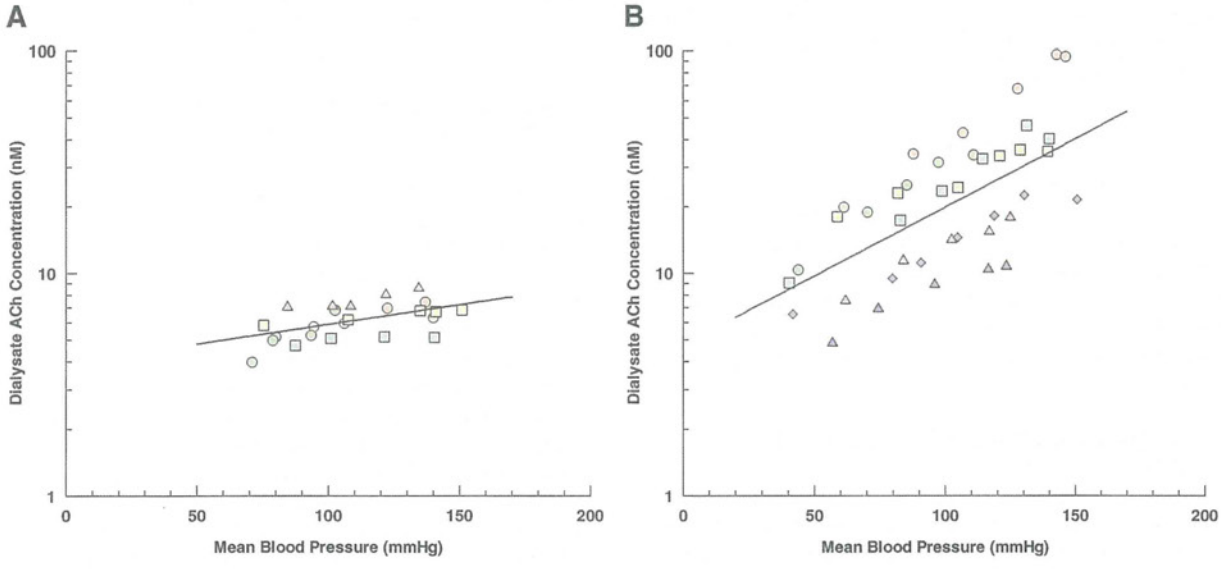

Figure 5. Regression lines of dialysate ACh concentration vs. MBP in control group (**A**) and medetomidine-treated group (**B**). In the control group (n=5), the increase in MBP had little effect on dialysate ACh concentration (**A**). In the medetomidine-treated group (n=7), dialysate ACh concentration was elevated with increase in MBP (**B**). Average regression line for control group: log[ACh]= 0.0018×MBP+0.59. Average regression line for medetomidine-treated group: log[ACh]=0.0062×MBP+0.68. Each symbol represents the data of 1 animal. ACh, acetylcholine; MBP, mean blood pressure.

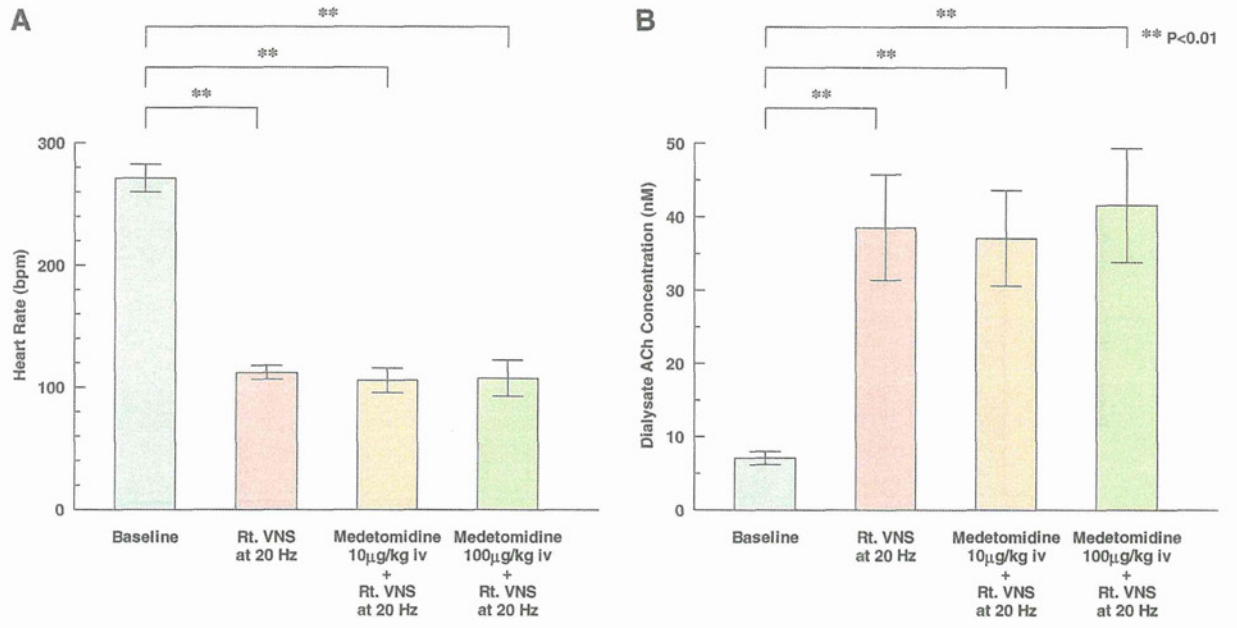

Figure 6. Peripheral effects of medetomidine on heart rate (**A**) and dialysate acetylcholine (ACh) concentration (**B**) under electrical stimulation of the right cervical vagal nerve. The 20-Hz electrical stimulation of the right cervical vagal nerve significantly decreased heart rate and increased dialysate ACh concentration. However, medetomidine did not affect the heart rate and dialysate ACh concentration under electrical vagal nerve stimulation (VNS).

detomidine did not affect heart rate and dialysate ACh concentration under the electrical stimulation (106±9.9 beats/min and 37.1±6.1 nmol/L at 10 μg/kg, 108±15 beats/min and 41.6±7.7 nmol/L at 100 μg/kg).

Discussion

We have elucidated the effects of medetomidine on cardiac sympathetic and vagal nerve activities simultaneously using cardiac microdialysis technique. Intravenous administration of 10 μg/kg of medetomidine significantly decreased sympathetic NE release to the SA node, while intravenous administration of 100 μg/kg of medetomidine significantly increased vagal ACh release to the SA node in addition to sympathetic suppression.

α_2-Adrenergic Agonist and Cardiac Sympathetic Nerve Activity

It is well-documented that α_2-adrenergic agonist suppresses sympathetic nerve activity.[15] Oku et al reported that dexmedetomidine suppressed renal sympathetic nerve discharge in baroreceptor-denervated rabbits.[16] In the present study, low-dose medetomidine decreased heart rate and mean BP through inhibiting sympathetic nerve activity, without affecting cardiac vagal nerve activity. High-dose medetomidine also suppressed NE release to the same level as low-dose medetomidine.

Several mechanisms may be involved in the sympathoinhibitory effect of α_2-adrenergic agonist. The rostral ventrolateral medulla has been reported to serve as an important site in mediating the hypotensive and sedative effects of α_2-adrenergic agonist.[17] McCallum et al reported that the central sympathoinhibitory effects of α_2-adrenoceptor stimulation are augmented by peripheral inhibition of ganglionic transmission.[18] The results obtained from protocol 1 indicate that low-dose medetomidine may induce a vagal-dominant condition through suppression of the cardiac sympathetic nerve without direct activation of the cardiac vagal nerve.

α_2-Adrenergic Agonist and Cardiac Vagal Nerve Activity

Kamibayashi et al reported that the vagus nerve played an important role in the antidysrhythmic effect of dexmedetomidine.[3] However, because it is difficult to selectively monitor cardiac vagal nerve activity, there is little direct evidence that α_2-adrenergic agonists can directly increase cardiac vagal nerve activity. In the present study, high-dose medetomidine significantly decreased heart rate and mean BP compared with low-dose medetomidine in protocol 1, and analyses of NE and ACh release by microdialysis technique proved that these decreases in heart rate and mean BP were associated with an increase in vagal ACh release to the heart. Histocytological studies demonstrated the presence of α_2-adrenergic receptors in the vagal dorsal motor nucleus and nucleus tractus solitarius.[19] Therefore, it is possible that α_2-adrenergic agonists directly activate the cardiac vagal nerve. It is also possible that intravenous medetomidine also modulates vagal ACh release through ganglionic transmission and the direct action to nerve endings. In protocol 4, however, medetomidine did not affect heart rate or the dialysate ACh concentration under electrical stimulation of the right efferent vagal nerve. Thus, in our experimental setting the peripheral effects of medetomidine on cardiac vagal nerve activity may be small compared with its central effects.

To exclude the possibility that medetomidine-induced hypotension affects local ACh concentrations, the mean BP was maintained constant by co-administration of phenylephrine in protocol 2. High-dose medetomidine combined with phenylephrine enhanced the decrease in heart rate and the increase in dialysate ACh concentration without medetomi-

dine-induced hypotension, indicating that hypotension occurring in protocol 1 had actually reduced ACh release in response to high-dose medetomidine. The results also suggest an interaction between baroreflex-induced and medetomidine-induced vagal nerve activation, which was extensively examined in protocol 3. In protocol 3, medetomidine steepened the slope of the regression line between mean BP and log dialysate ACh concentration, without affecting the intercept. In other words, medetomidine enhanced the baroreflex-induced ACh release from cardiac vagal nerve endings. Because the central pathway of baroreflex includes the vagal dorsal motor nucleus and nucleus tractus solitarius, in which α_2-adrenergic receptors have been demonstrated,[19] medetomidine may act on this pathway and modulate baroreflex-induced ACh release.

Clinical Implication

The selective α_2-adrenergic agonist, dexmedetomidine, is widely used for sedation in intensive care units. Bradycardia and hypotension are known to be unfavorable events during dexmedetomidine sedation.[20] Some cases of dexmedetomidine-induced atrioventricular block followed by cardiac arrest have been reported.[21,22] This critical complication may be associated with direct vagal activation by the α_2-adrenergic agonist. Compared with our previous results of electrical cervical vagal nerve stimulation in rabbits,[9] intravenous administration of 100 μg/kg of medetomidine had an effect equivalent to electrical vagal stimulation at 10 Hz. Furthermore, when the mean BP was maintained constant using phenylephrine, medetomidine had a stronger effect on cardiac vagal nerve activity, which is similar to 20-Hz electrical vagal stimulation, and this magnitude may sometimes cause atrioventricular block or sinus arrest.

Notwithstanding these adverse effects, vagal activation has several favorable cardioprotective effects. Our study proved that medetomidine, a selective α_2-adrenergic agonist, is a strong activator of cardiac vagal nerve. Vanoli et al[6] reported that vagal stimulation after acute ischemia can prevent ventricular fibrillation. Ando et al reported that efferent vagal nerve stimulation prevented ischemia-induced arrhythmias by preserving connexin 43 protein.[23] Our results suggest that vagal activation in addition to sympathetic suppression probably contributes to the antiarrhythmic effect of medetomidine.

Because inhibition of the sympathetic nerve system has been the cornerstone of drug therapy for heart failure,[24] a selective α_2-adrenergic agonist may be a potential therapeutic option for heart failure. Recent studies have shown that electrical vagal nerve stimulation also improves the outcomes in patients with heart failure.[25] Electrical stimulation of carotid baroreceptor has recently been reported to be a therapeutic option for heart failure. Sabbah et al reported that chronic electrical stimulation of the carotid sinus baroreflex improved left ventricular function and promoted reversal of ventricular remodeling in dogs with advanced heart failure.[26] Our study demonstrated that medetomidine modulates baroreflex control to enhance vagal nerve activity, which may also induce further cardioprotective effects.

Study Limitations

First, ACh is degraded by ACh esterase immediately after release. Therefore, detection of in vivo ACh release requires the addition of eserine, a specific ACh esterase inhibitor, into the perfusate. The presence of eserine around the semipermeable membrane might have affected ACh release in the vicinity of the semipermeable membrane. Eserine could have activated regulatory pathways such as autoinhibition of ACh release via muscarinic receptors.

Second, medetomidine is a chiral imidazole derivative. Thus, imidazoline receptors may also be involved in the cardiac vagal activation by medetomidine. Further investigation is necessary to clarify the influence of imidazoline receptors on cardiac vagal nerve activity. However, because an α_2-adrenergic antagonist, atipamezole, abolished the hemodynamic responses to medetomidine, we think that the cardiovascular effects of medetomidine are mainly related to the direct action of α_2-adrenergic receptors.

Third, the interactive effects between sympathetic and vagal nerve endings remain uncertain in the present study. Thus, we need further investigations including the open-loop approach where baroreceptor input pressure is strictly controlled.

Conclusion

A selective α_2-adrenergic agonist, medetomidine, directly activates cardiac vagal nerve and enhances the baroreflex control of vagal nerve activity. Medetomidine may be a therapeutic option for life-threatening arrhythmia or heart failure if the adverse effects are properly managed.

Acknowledgments

This study was supported by a research project promoted by the Japanese Ministry of Health, Labour and Welfare (H20-katsudo-Shitei-007 and H21-nano-Ippan-005); Grants-in-Aid for Scientific Research (No. 20390462 and No. 23592319) from the Ministry of Education, Culture, Sports, Science and Technology; the Industrial Technology Research Grant Program from New Energy and Industrial Technology Development Organization (NEDO) of Japan; and Dr Hiroshi Irisawa & Dr Aya Irisawa Memorial Research Grant from the Japan Heart Foundation.

References

1. Hsu YW, Cortinez LI, Robertson KM, Keifer JC, Sum-Ping ST, Moretti EW, et al. Dexmedetomidine pharmacodynamics: Part I: Crossover comparison of the respiratory effects of dexmedetomidine and remifentanil in healthy volunteers. *Anesthesiology* 2004; **101:** 1066–1076.
2. Hayashi Y, Sumikawa K, Maze M, Yamatodani A, Kamibayashi T, Kuro M, et al. Dexmedetomidine prevents epinephrine-induced arrhythmias through stimulation of central alpha 2 adrenoceptors in halothane-anesthetized dogs. *Anesthesiology* 1991; **75:** 113–117.
3. Kamibayashi T, Hayashi Y, Mammoto T, Yamatodani A, Sumikawa K, Yoshiya I. Role of the vagus nerve in the antidysrhythmic effect of dexmedetomidine on halothane/epinephrine dysrhythmias in dogs. *Anesthesiology* 1995; **83:** 992–999.
4. Yamazaki T, Asanoi H, Ueno H, Yamada K, Takagawa J, Kameyama T, et al. Central sympathetic inhibition augments sleep-related ultradian rhythm of parasympathetic tone in patients with chronic heart failure. *Circ J* 2005; **69:** 1052–1056.
5. Lombardi F, Sandrone G, Pernpruner S, Sala R, Garimoldi M, Cerutti S, et al. Heart rate variability as an index of sympathovagal interaction after acute myocardial infarction. *Am J Cardiol* 1987; **60:** 1239–1245.
6. Vanoli E, De Ferrari GM, Stramba-Badiale M, Hull SS Jr, Foreman RD, Schwartz PJ. Vagal stimulation and prevention of sudden death in conscious dogs with a healed myocardial infarction. *Circ Res* 1991; **68:** 1471–1481.
7. Schwartz PJ, La Rovere MT, Vanoli E. Autonomic nervous system and sudden cardiac death: Experimental basis and clinical observations for post-myocardial infarction risk stratification. *Circulation* 1992; **85:** I77–I91.
8. Kuusela E, Raekallio M, Anttila M, Falck I, Mölsä S, Vainio O. Clinical effects and pharmacokinetics of medetomidine and its enantiomers in dogs. *J Vet Pharmacol Ther* 2000; **23:** 15–20.
9. Shimizu S, Akiyama T, Kawada T, Shishido T, Yamazaki T, Kamiya A, et al. In vivo direct monitoring of vagal acetylcholine release to the sinoatrial node. *Auton Neurosci* 2009; **148:** 44–49.
10. Shimizu S, Akiyama T, Kawada T, Shishido T, Mizuno M, Kamiya A, et al. In vivo direct monitoring of interstitial norepinephrine levels at the sinoatrial node. *Auton Neurosci* 2010; **152:** 115–118.
11. Shimizu S, Akiyama T, Kawada T, Sonobe T, Kamiya A, Shishido T, et al. Centrally administered ghrelin activates cardiac vagal nerve

in anesthetized rabbits. *Auton Neurosci* 2011; **162:** 60–65.
12. Akiyama T, Yamazaki T, Ninomiya I. In vivo monitoring of myocardial interstitial norepinephrine by dialysis technique. *Am J Physiol* 1991; **261:** H1643–H1647.
13. Akiyama T, Yamazaki T, Ninomiya I. In vivo detection of endogenous acetylcholine release in cat ventricles. *Am J Physiol* 1994; **266:** H854–H860.
14. Glantz SA. Primer of biostatistics, 6th edn. New York: McGraw-Hill, 2005.
15. Heusch G, Schipke J, Thämer V. Clonidine prevents the sympathetic initiation and aggravation of poststenotic myocardial ischemia. *J Cardiovasc Pharmacol* 1985; **7:** 1176–1182.
16. Oku S, Benson KT, Hirakawa M, Goto H. Renal sympathetic nerve activity after dexmedetomidine in nerve-intact and baroreceptor-denervated rabbits. *Anesth Analg* 1996; **83:** 477–481.
17. Yamazato M, Sakima A, Nakazato J, Sesoko S, Muratani H, Fukiyama K. Hypotensive and sedative effects of clonidine injected into the rostral ventrolateral medulla of conscious rats. *Am J Physiol Regul Integr Comp Physiol* 2001; **281:** R1868–R1876.
18. McCallum JB, Boban N, Hogan Q, Schmeling WT, Kampine JP, Bosnjak ZJ. The mechanism of alpha2-adrenergic inhibition of sympathetic ganglionic transmission. *Anesth Analg* 1998; **87:** 503–510.
19. Robertson HA, Leslie RA. Noradrenergic alpha 2 binding sites in vagal dorsal motor nucleus and nucleus tractus solitarius: Autoradiographic localization. *Can J Physiol Pharmacol* 1985; **63:** 1190–1194.
20. Candiotti KA, Bergese SD, Bokesch PM, Feldman MA, Wisemandle W, Bekker AY; MAC Study Group. Monitored anesthesia care with dexmedetomidine: A prospective, randomized, double-blind, multicenter trial. *Anesth Analg* 2010; **110:** 47–56.
21. Nagasaka Y, Machino A, Fujikake K, Kawamoto E, Wakamatsu M. Cardiac arrest induced by dexmedetomidine. *Masui* 2009; **58:** 987–989.
22. Ingersoll-Weng E, Manecke GR Jr, Thistlethwaite PA. Dexmedetomidine and cardiac arrest. *Anesthesiology* 2004; **100:** 738–739.
23. Ando M, Katare RG, Kakinuma Y, Zhang D, Yamasaki F, Muramoto K, et al. Efferent vagal nerve stimulation protects heart against ischemia-induced arrhythmias by preserving connexin43 protein. *Circulation* 2005; **112:** 164–170.
24. Sata Y, Krum H. The future of pharmacological therapy for heart failure. *Circ J* 2010; **74:** 809–817.
25. Schwartz PJ. Vagal stimulation for heart diseases: From animals to men: An example of translational cardiology. *Circ J* 2010; **75:** 20–27.
26. Sabbah HN, Gupta RC, Imai M, Irwin ED, Rastogi S, Rossing MA, et al. Chronic electrical stimulation of the carotid sinus baroreflex improves left ventricular function and promotes reversal of ventricular remodeling in dogs with advanced heart failure. *Circ Heart Fail* 2011; **4:** 65–70.

J Appl Physiol 111: 1614–1621, 2011.
First published September 15, 2011; doi:10.1152/japplphysiol.00501.2011.

Interaction between vestibulo-cardiovascular reflex and arterial baroreflex during postural change in rats

Chikara Abe,[1] Toru Kawada,[2] Masaru Sugimachi,[2] and Hironobu Morita[1]

[1]*Department of Physiology, Gifu University Graduate School of Medicine, Gifu; and* [2]*Department of Cardiovascular Dynamics, National Cerebral and Cardiovascular Center Research Institute, Suita, Japan*

Submitted 25 April 2011; accepted in final form 8 September 2011

Abe C, Kawada T, Sugimachi M, Morita H. Interaction between vestibulo-cardiovascular reflex and arterial baroreflex during postural change in rats. *J Appl Physiol* 111: 1614–1621, 2011. First published September 15, 2011; doi:10.1152/japplphysiol.00501.2011.—To examine a cooperative role for the baroreflex and the vestibular system in controlling arterial pressure (AP) during voluntary postural change, AP was measured in freely moving conscious rats, with or without sinoaortic baroreceptor denervation (SAD) and/or peripheral vestibular lesion (VL). Voluntary rear-up induced a slight decrease in AP (−5.6 ± 0.8 mmHg), which was significantly augmented by SAD (−14.7 ± 1.0 mmHg) and further augmented by a combination of VL and SAD (−21 ± 1.0 mmHg). Thus we hypothesized that the vestibular system sensitizes the baroreflex during postural change. To test this hypothesis, open-loop baroreflex analysis was conducted on anesthetized sham-treated and VL rats. The isolated carotid sinus pressure was increased stepwise from 60 to 180 mmHg while rats were placed horizontal prone or in a 60° head-up tilt (HUT) position. HUT shifted the carotid sinus pressure-sympathetic nerve activity (SNA) relationship (neural arc) to a higher SNA, shifted the SNA-AP relationship (peripheral arc) to a lower AP, and, consequently, moved the operating point to a higher SNA while maintaining AP (from 113 ± 5 to 114 ± 5 mmHg). The HUT-induced neural arc shift was completely abolished in VL rats, whereas the peripheral arc shifted to a lower AP and the operating point moved to a lower AP (from 116 ± 3 to 84 ± 5 mmHg). These results indicate that the vestibular system elicits sympathoexcitation, shifting the baroreflex neural arc to a higher SNA and maintaining AP during HUT.

arterial baroreflex; arterial pressure; sympathetic nerve activity; head-up tilt; rear-up; neural arc; peripheral arc

DAILY ACTIVITY-INDUCED CHANGES in the gravitational vector are one of the major disturbances that affect the cardiovascular system (43). For example, a postural change from a recumbent to an upright position induces an increase in the hydrostatic pressure gradient, a footward fluid shift, reduced venous return and cardiac output, and reduced arterial pressure (AP). This reduction in AP is sensed by baroreceptors in the blood vessels, and AP is thought to be stabilized by the arterial baroreflex, an important negative feedback process (6, 37). Alternatively, postural changes might stimulate the vestibular organ, which is also thought to be involved in AP regulation with postural change (8, 17, 30, 39). AP maintenance during passive postural change was found to be dependent on the vestibular system: if the vestibular system was not functioning properly, AP decreased or fluctuated. However, the role of the vestibular system in maintaining AP during a voluntary postural change remains unclear, since most previous experiments studied passive postural change using a tilt table. Therefore, one of the aims of this study was to examine the role of the vestibular system in maintaining AP during a voluntary postural change in conscious rats. This is important for considering the role of the vestibular system in maintaining AP during daily activity. We tested the hypothesis that the vestibular system plays a significant role in AP maintenance during voluntary rear-up behavior in rats.

Stimulation of the vestibular system by head movement or changes in gravitational forces is known to induce sympathoexcitation (2, 11, 23, 33). Although sympathoexcitation was observed during postural change (10, 18, 31), it is not clear whether it is mediated through the vestibular system. Postural change-induced AP decrease might also induce sympathoexcitation through the arterial baroreflex. In this regard, Ray (33) performed an elegant experiment demonstrating that lower body negative pressure, which is a result of postural change-induced footward fluid shift, induces an increase in sympathetic nerve activity (SNA); a further increase in SNA was observed by head-down rotation. This result strongly suggests that the observed sympathoexcitation upon postural change might be a sum of the baroreflex-mediated and the vestibular-mediated sympathoexcitation. Thus it is possible that vestibular-mediated sympathoexcitation modulates arterial baroreflex function during postural change. Anatomic and functional convergence of vestibular and baroreceptor signaling to the nucleus tractus solitarius further supports the idea of interaction between the vestibular system and arterial baroreflex (4, 28, 45). However, functional interaction between the baroreflex and the vestibular system during postural change has not been quantitatively analyzed. Therefore, the second aim of the present study was to quantitatively analyze the functional interaction between the baroreflex and the vestibular system during postural change. We tested the hypothesis that the vestibulo-sympathetic reflex sensitizes the arterial baroreflex during postural change.

To address the first aim, the AP response during voluntary rear-up behavior was measured in rats with or without a peripheral vestibular organ and/or arterial baroreceptors. To address the second aim, we evaluated the arterial baroreflex functional curve in an open-loop experiment with isolated carotid sinus baroreceptor regions during prone and 60° head-up tilt (HUT) positions in sham-treated vestibular-intact (sham) and vestibular-lesioned (VL) rats.

METHODS

Animals. The animals used in the study were maintained in accordance with the "Guiding Principles for the Care and Use of Animals in the Field of Physiological Science" set by the Physiological Society of Japan. The experiments were approved by the Animal Research

Address for reprint requests and other correspondence: H. Morita, Dept. of Physiology, Gifu Univ. Graduate School of Medicine, 1-1 Yanagido, Gifu 501-1194, Japan (e-mail: zunzunmorita@gmail.com).

Committee of Gifu University and by the Animal Subjects Committee of the National Cerebral and Cardiovascular Center, Japan. Male Sprague-Dawley rats ($n = 42$), weighing 230–250 g (8 wk old), were used for the experiments.

AP measurement in conscious rats. To examine the role of the vestibular system and/or sinoaortic baroreflex in AP regulation during voluntary rear-up behavior, AP was continuously measured for 48 h in chronically implanted conscious rats. Four groups of rats were examined: sham group ($n = 7$), in which both the sinoaortic baroreceptors and vestibular organs were intact; VL group ($n = 7$), in which the sinoaortic baroreceptors were intact, but the vestibular organs were lesioned; sinoaortic baroreceptor denervation (SAD) group ($n = 7$), in which the sinoaortic baroreceptors were denervated, but the vestibular organs were intact; and SAD+VL group ($n = 7$), in which both the sinoaortic baroreceptors and vestibular organs were lesioned. The following operations were performed to prepare these groups of rats.

Ten days before the experiment, all rats were anesthetized with pentobarbital sodium (50 mg/kg), and the following operations were performed. *1*) The abdominal aorta was exposed via a midline laparotomy for rats in all groups. The catheter portion of the telemetry transmitter probe for AP measurements (PA-C40; Data Science International, St Paul, MN) was inserted into the abdominal aorta. The tip of the catheter was set distal to the renal artery bifurcation. The probe was then sutured to the abdominal wall, and the incision was closed. *2*) In the VL and SAD+VL rats, sodium arsanilate solution (100 mg/ml) was injected into the bilateral middle ear cavities (50 μl/ear). Although the histological verification was not performed in the present study, previous study from our laboratory has proved that this VL method could completely destroy the epithelial cells (1). As a control, saline, instead of sodium arsanilate solution, was injected into the sham and SAD rats. *3*) In the SAD and SAD+VL rats, the aortic depressor nerve was isolated and dissected with a midcervical incision, the carotid sinus was isolated from the surrounding connective tissues, and 10% phenol in ethanol was applied. In the sham and VL rats, a midcervical incision was made, but the aortic depressor nerves and carotid sinus were left intact as a control. *4*) A polyethylene catheter (PE-50; Becton Dickinson, Sparks, MD) was inserted into the inferior vena cava via the left femoral vein to confirm the completeness of SAD using a phenylephrine injection 2 days after surgery. In rats with SAD, phenylephrine-induced bradycardia was completely abolished. This polyethylene catheter was removed after the confirmation of SAD under gas anesthesia with enflurane (Abbott Japan, Osaka, Japan).

All of the rats were maintained in their individual cages to recover from surgery until the day of the experiment. Penicillin G potassium (6,000 U/day) and buprenorphine (3 μg/kg) were injected intramuscularly for 3 days after surgery. At 5 days postsurgery, the swimming test was performed to confirm the completion of VL. Rats were gently put on the surface of tepid water, and swimming behavior was observed. Sham rats could swim and reached the edge of water bath (27 cm width × 40 cm length × 20 cm depth); however, VL rats were unable to determine the direction in which they had to swim to reach the water surface and continued to turn around under the water (14).

On the day of the experiment, each rat was placed in an individual cage (20 cm width × 36 cm length × 22 cm height). Infrared sensors (NA2-N16D; SUNX, Aichi, Japan) were aligned horizontally at a height of 15 cm from the floor of the cage. The AP signal was received by a PhysioTel Receiver (RLA 1020; Data Science International), and the output was relayed through a calibrated pressure output adapter (R11CPA; Data Science International) and a dual ambient pressure monitor (C11PR; Data Science International). The AP and the signal from the infrared sensor were recorded using an analog-to-digital converter (PowerLab; AD instruments, Bella Vista, NSW, Australia) at a rate of 100 Hz. Video pictures from a video camera (DCR-TRV70; Sony, Tokyo, Japan) were also synchronized with the digital data. All of the rats were fed ad libitum, the cages were maintained on a 12:12-h light-dark cycle, and the room temperature was maintained at 24 ± 1°C. If the infrared signal was on for more than 15 s, the video picture was checked to see whether that behavior was related to drinking, because drinking behavior itself affects AP (13, 41). We defined rear-up behavior as rear-up (>15 s) without drinking. The minimum number of rear-ups lasting for more than 15 s was 30 for two SAD+VL rats; therefore, we randomly selected 30 rear-up events (Rnd function of Excel VBA) for each rat in all groups, and these data were averaged.

Measurement of baroreflex gain under open-loop conditions. Operations to generate the sham ($n = 7$) and VL ($n = 7$) rats were performed 5 days before the experiment. Anesthesia was induced using enflurane (Abbott Japan, Osaka, Japan) inhalation via a face mask. Sodium arsanilate solution (100 mg/ml) or saline was injected into the bilateral middle ear cavities (50 μl/ear) of VL and sham rats, respectively. Penicillin G potassium (6,000 U/day) was injected intramuscularly for 3 days after surgery.

On the day of the experiment, each rat was anesthetized with an intraperitoneal injection (2 ml/kg) of a mixture of urethane (500 mg/ml) and α-chloralose (50 mg/ml) and mechanically ventilated (SAR830/P; CWE, Ardmore, PA) through a tracheal tube with oxygen-enriched room air. A venous catheter was inserted into the left femoral vein, and a mixed solution [1 ml of the mixed urethane and α-chloralose solution, 2 ml of pancuronium bromide (Myoblock, Sankyo, Tokyo, Japan), and 47 ml of Ringer solution] was administered continuously (5 $ml \cdot kg^{-1} \cdot h^{-1}$). An arterial catheter was inserted into the left femoral artery to measure AP. Heart rate (HR) was calculated from the AP waveform. To record SNA, the postganglionic renal sympathetic nerve was isolated through a right or left flank incision, and two stainless-steel electrodes (AS633; Cooner Wire, Chatsworth, CA) were placed around it. The nerve and electrodes were covered and fixed with silicone gel (Kwik-Sil; World Precision Instruments).

The vagal and aortic nerves were sectioned bilaterally at the neck, avoiding the reflexes from the cardiopulmonary region and the aortic arch. The carotid sinus regions were isolated bilaterally from the systemic circulation, according to previously reported procedures (36, 38). Briefly, a 7–0 polypropylene suture with a fine needle (Prolene, Ethicon) was passed through the tissue between the external and internal carotid arteries, and the external carotid artery was ligated close to the carotid bifurcation. The internal carotid artery was embolized with two to three steel balls (0.8 mm diameter; Tsubaki Nakashima, Nara, Japan) injected into the common carotid artery. Under these conditions, the brain stem area was perfused using the bilateral vertebral arteries. The isolated carotid sinuses were filled with warmed Ringer solution through catheters inserted into the common carotid arteries. Carotid sinus pressure (CSP) was regulated with a servo-controlled piston pump. Heparin sodium (100 U/kg) was given intravenously to prevent blood coagulation. Body temperature was maintained at ~37°C with a heating pad.

After the surgical procedures were completed, the rat was fixed on a tilt table with the maxillary incisal teeth anchor. All signals were recorded using an analog-to-digital converter (PowerLab; AD instruments) at a rate of 1,000 Hz. To estimate the static input-output relationship of the carotid sinus baroreflex, the CSP was set to 60 mmHg for 4–6 min and then increased stepwise from 60 to 180 mmHg in increments of 20 mmHg per 30 s. This procedure was repeated three times in the prone horizontal position and three times in the HUT position. At the end of the experiment, we confirmed the disappearance of SNA in response to an intravenous bolus injection of a ganglionic blocker, hexamethonium bromide (60 mg/kg), and recorded the noise level, which was treated as the zero level of SNA. Because the absolute voltage of SNA varied among the animals, depending on the recording conditions, the average SNA during the last 10 s at a CSP level of 60 mmHg in the prone horizontal position was defined as 100%. To quantify the open-loop static characteristics of the carotid sinus baroreflex, the mean SNA and AP were obtained during the last 10 s at each CSP level of the stepwise input protocol.

Table 1. *Means ± SE for AP, HR, and AP variability for each group*

Group	*n*	AP, mmHg	HR, beats/min	Variability, mmHg
Sham	7	96 ± 2	412 ± 4	7.1 ± 0.4
VL	7	97 ± 2	409 ± 3	7.4 ± 0.2
SAD	7	96 ± 3	403 ± 2	18.5 ± 1.2*
SAD+VL	7	97 ± 1	408 ± 4	17.8 ± 0.7*

Values are means ± SE; *n*, no. of rats. Arterial pressure (AP) and heart rate (HR) were measured for 12 h and averaged every 5 s to obtain individual baseline values and then averaged to obtain the group mean ± SE. Variability is the standard deviation of AP. Sham, vestibular intact; VL, vestibular lesioned; SAD, sinoaortic baroreceptor denervated. *$P < 0.05$ vs. sham or VL.

The static characteristics of the baroreflex neural arc (relationship between CSP and SNA) and the total baroreflex (relationship between CSP and AP) were described by fitting four-parameter logistic functions to the input-output data as follows (20, 22):

$$y = P_1/\{1 + \exp[P_2 \times (x - P_3)]\} + P_4$$

where x and y denote the input (CSP) and output (SNA or AP), respectively; P_1 is the response range of the output; P_2 is the slope coefficient; P_3 is the midpoint pressure of the input; and P_4 is the minimum value for the output. For convenience, the maximum gain of the logistic function is reported by a positive value as $P_1 \times P_2/4$.

The static characteristics of the baroreflex peripheral arc (relationship between SNA and AP) were quantified from a scatter plot. A linear regulation line is represented as follows:

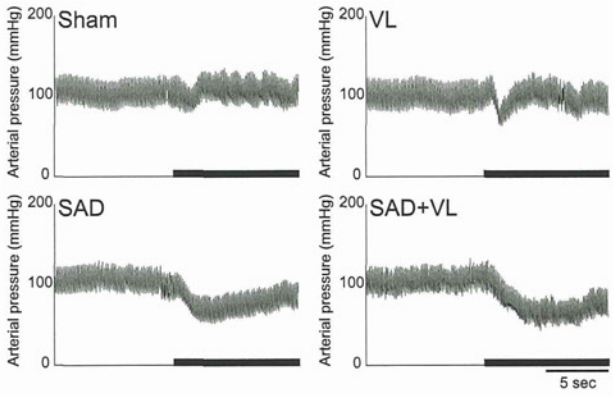

Fig. 2. Typical recordings of arterial pressure (AP) in response to rear-up in vestibular-intact (sham), VL, SAD, and SAD+VL rats. The thick horizontal bar indicates the rear-up period.

$$AP = a \times SNA + b$$

where a and b represent the slope and intercept, respectively.

Statistical analysis. All data are presented as means ± SE. For the data presented in Table 1 and Fig. 3*B*, one-way ANOVA was applied. Repeated-measures two-way ANOVA was used for the data presented in Table 2. If the *F*-ratio indicated statistical significance, the Tukey-Kramer post hoc test was applied for between-group comparisons. A simple linear regression line was calculated using the least squares method for the peripheral arc of Fig. 5*B*, and the analysis of covari-

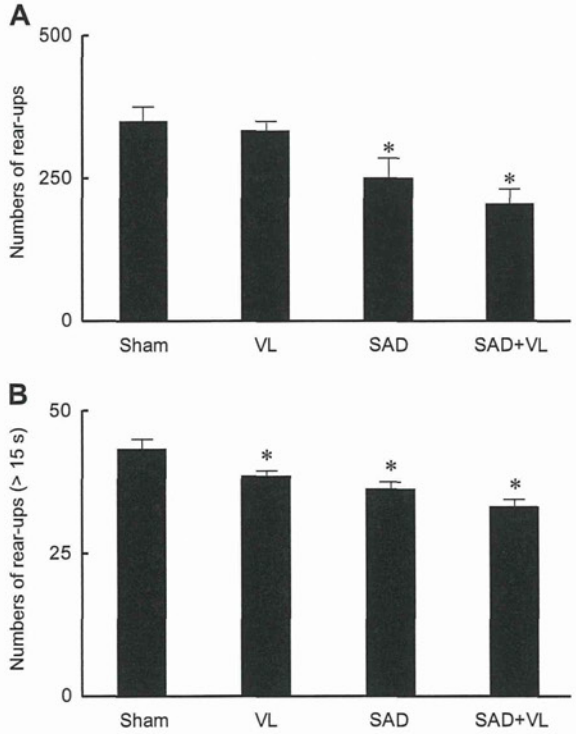

Fig. 1. Summarized data for the total number of rear-ups without drinking during the 12-h dark period (*A*), and rear-ups lasting for more than 15 s (*B*) in the sham-treated (sham), vestibular-lesioned (VL), sinoaortic baroreceptor-denervated (SAD), and SAD+VL rats. Values are means ± SE. *$P < 0.05$ vs. sham.

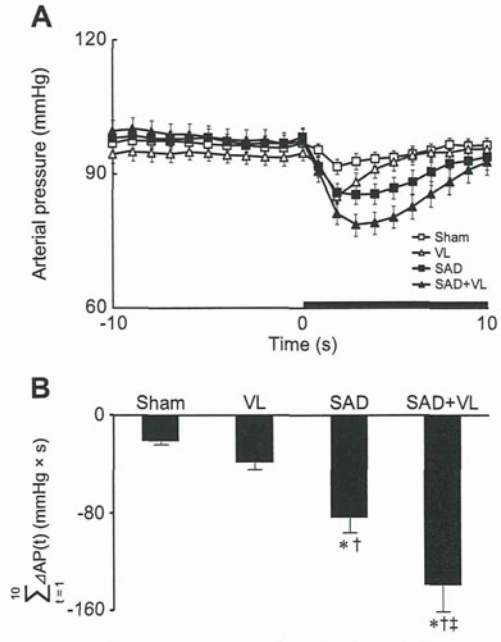

Fig. 3. *A*: average AP response to rear-up behavior in vestibular-intact (sham), VL, SAD, and SAD+VL rats. Thirty data points measuring AP induced by rear-up exceeding 15 s were randomly selected from the individual rats and then averaged for each group. The thick horizontal bar indicates the rear-up period. *B*: summarized data for the sum of the differences in AP ($\sum\Delta AP$) between each time point (t; 1–10 s) during rear-up and the mean value for the 10 s before rear-up. If the difference was positive, the value was considered to be zero. Values are means ± SE. *$P < 0.05$ vs. sham rats. †$P < 0.05$ vs. VL rats. ‡$P < 0.05$ vs. SAD rats.

ance method was applied. In all tests, $P < 0.05$ was considered statistically significant.

RESULTS

To determine whether the vestibular system and/or sinoaortic baroreflex is required for AP regulation during voluntary rear-up behavior, the AP of sham, SAD, VL, and SAD+VL rats was measured. Table 1 shows the mean baseline AP, HR, and AP variability of all of the groups in the experiment. Baseline AP and HR were measured for the 12-h dark period and averaged every 5 s. AP variability is the standard deviation of AP for the 12 h of the dark period. There were no differences in baseline AP or HR among the groups, but a significant increase in AP variability was observed in the SAD and SAD+VL rats compared with both sham and VL rats.

Although there was no obvious difference in the rear-up behavior among groups (supplemental video file; the online version of this article contains supplemental data), the number of rear-ups was affected in the VL and SAD+VL rats compared with sham (Fig. 1*A*). The sham and VL rats reared up ~350 times during the 12-h dark period, which was significantly reduced in the SAD and SAD+VL rats. Furthermore, the number of rear-ups lasting more than 15 s was significantly reduced in the VL, SAD, and SAD+VL rats compared with sham rats (Fig. 1*B*).

Figure 2 shows typical recordings of AP during rear-up behavior in sham, VL, SAD, and SAD+VL rats. AP response during rear-up behavior is summarized in Fig. 3 for all groups. In the sham rats, AP levels changed very little during rear-up (-5.6 ± 0.8 mmHg; Fig. 3*A*). A transient drop in AP (-9.4 ± 0.6 mmHg) was observed at the onset of rear-up in VL rats, but values quickly recovered to the baseline level. In the SAD rats, the reduction in AP was large (-14.7 ± 1.0 mmHg), and recovery was delayed. This tendency was clearly seen in the SAD+VL rats, in which AP decreased by 21 ± 1.0 mmHg, and its recovery was delayed. For statistical analysis, the sum of the differences ($\sum\Delta$) between the 10-s averaged data before rear-up and at each time point during rear-up (from 1 to 10 s) was calculated (Fig. 3*B*). SAD significantly increased $\sum\Delta$AP compared with the sham rats. VL alone had no significant effect on $\sum\Delta$AP, whereas additional VL to SAD significantly increased $\sum\Delta$AP compared with the SAD rats. $\sum\Delta$AP in the SAD+VL rats (131 mmHg × s) was greater than the simple sum of $\sum\Delta$AP in VL and SAD (111 mmHg × s).

Typical recordings of the measurement of baroreflex gain under open-loop conditions are shown in Fig. 4. A stepwise increase in CSP reduced AP, HR, and SNA in both the prone and HUT positions in sham rats. When CSP was 60 mmHg, an increase in SNA was observed in a sham rat, but not in a VL rat.

Figure 5 summarizes the open-loop static characteristics of the carotid sinus baroreflex in the sham and VL rats in the prone and HUT positions. Each parameter is summarized in Table 2. Figure 5*A* shows the baroreflex neural arc of the sham and VL rats in the prone and HUT positions. In the sham rats, the response range of SNA (P_1) was significantly increased by HUT, but the minimum SNA (P_4) did not change, so the increase in the response range was mainly directed to a higher SNA level. SNA levels were similar in VL rats in the prone and HUT positions. Therefore, the response range in the sham HUT

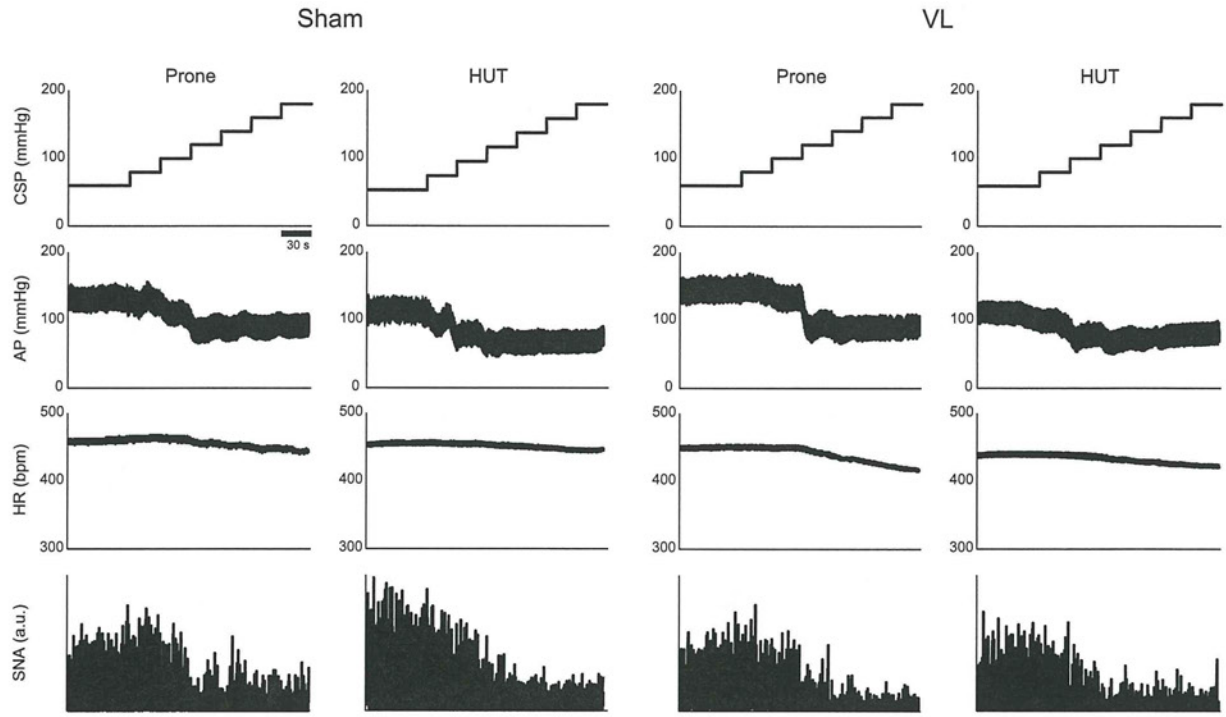

Fig. 4. Representative recordings of the carotid sinus pressure (CSP), AP, heart rate (HR), and renal sympathetic nerve activity (SNA) in vestibular-intact (sham) and VL rats in prone and head-up tilt (HUT) positions. bpm. Beats/min; a.u., arbitrary units.

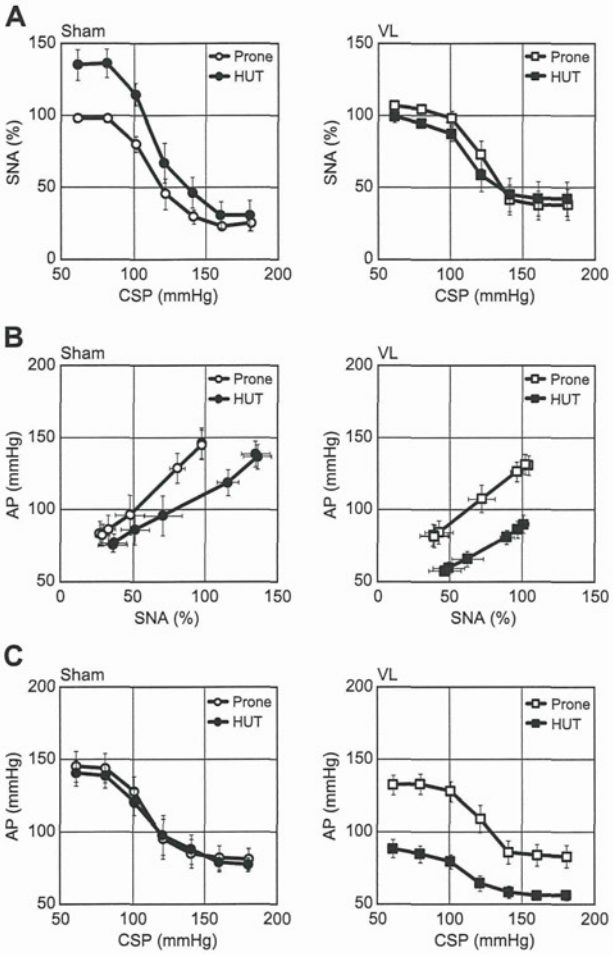

Fig. 5. Static characteristics of the average carotid sinus baroreflex for vestibular-intact (sham) and VL rats in the prone and HUT positions. Static characteristics of the baroreflex neural arc (*A*), baroreflex peripheral arc (*B*), and total baroreflex (*C*) are shown for sham (*left*) and VL (*right*) rats. Values are means ± SE.

rats was significantly larger than that in the VL HUT rats. Neither the maximum gain nor midpoint pressure was affected by VL or HUT (Table 2).

Analysis of covariance in the peripheral arc showed that there was no difference between the sham and VL rats in the prone position, whereas the line was shifted to a lower AP level during HUT in both the sham and VL rats (Fig. 5*B* and Table 2). The degree of shift was significantly larger in the VL rats than in the sham rats.

In the sham rats, the total baroreflex functional curve was not affected by HUT, nor was it affected by VL in the prone position (Fig. 5*C* and Table 2). However, HUT shifted the total functional curve to a lower AP level in the VL rats, with a significant reduction in the response range (P_1), minimum AP (P_4), and maximum gain.

The baroreflex equilibrium diagram was generated by plotting the neural and peripheral arcs on the pressure-SNA plane (Fig. 6). The ordinate is either CSP (the neural arc) or AP (the peripheral arc). The intersection between the neural and peripheral arcs gives the closed-loop operating points. The AP of the operating point was maintained in the sham rats during HUT, with an increase in SNA. In other words, the operating point shifted toward higher SNA levels, with maintenance of AP. However, in the VL rats, the operating point shifted to lower AP levels during HUT.

DISCUSSION

The major findings of the present study are as follows. *1*) The rear-up-induced reduction in AP was increased by SAD alone, but not VL alone; however, VL and SAD together significantly increased the rear-up-induced reduction in AP. *2*) The neural arc was shifted to a higher SNA level by HUT in the sham rats; this shift was not observed in the VL rats. *3*) A downward shift of the peripheral arc was observed in the sham and VL rats during HUT; the magnitude of this shift was greater in the VL rats than in the sham rats. *4*) The operating point of AP was maintained in the sham rats during HUT, but it was significantly reduced in the VL rats.

It is well accepted that the baroreflex plays a significant role in AP regulation during postural changes in humans and animals (9, 25, 37). However, the postural change-induced AP response in SAD animals is still controversial. In anesthetized SAD cats, a large and sustained reduction in AP was observed during HUT (6). In contrast, no difference in the AP response to rear-up behavior was observed between sham and SAD conscious rats (42). The difference in these two studies might be attributable to the use of anesthesia, passive or voluntary postural changes, and/or species differences. In the present study, a significantly larger reduction in AP was observed in conscious SAD rats than in sham rats. Two possibilities can be considered to explain this discrepancy. First, the AP response to rear-up with drinking was omitted from our data because drinking behavior increases AP (13, 41). Alternatively, the pressor response to drinking behavior may have obscured the depressor response to rear-up behavior in the SAD rats, as the drinking-behavior-induced pressor response was larger in the SAD rats than in the sham rats, because there was no buffering system (our unpublished data). Second, the AP variability in the SAD rats was 18.5 ± 1.2 mmHg in the present study, and this value is larger than that reported in the previous rat study (11.7 ± 1.5 mmHg) (42). It is possible that the quality of SAD was different between the two studies.

Passive HUT has been used to examine the role of the vestibular system in AP maintenance during postural changes (8, 17, 30, 39). The present study is the first to examine the role of the vestibular system in AP regulation during voluntary rear-up behavior, under which conditions the lower limb muscle is contracted. This muscle contraction might induce an increase in the venous return and then counteract rear-up-induced AP reduction (26). Furthermore, the muscle-contraction-induced proprioceptive reflex, the somatosensory reflex, and the behavior-linked central command might also counteract reduction in AP (5, 24, 27, 44). Under these conditions, VL alone had no significant effect on rear-up-induced AP reduction; however, in conjunction with an inoperable baroreflex, VL induced a larger reduction in AP compared with SAD alone. The reduction in AP seen in rats with VL or SAD alone was increased by additional denervation. Therefore, the vestibulo-cardiovascular reflex and the baroreflex might operate

Table 2. *Parameters representing the static characteristics of the carotid sinus baroreflex*

	Sham (n = 7)		VL (n = 7)	
	Prone	HUT	Prone	HUT
		Neural arc		
P_1, response range, %	70 ± 6	104 ± 15*	63 ± 8	53 ± 10†
P_2, slope coefficient, mmHg^{-1}	0.32 ± 0.15	0.14 ± 0.03	0.16 ± 0.02	0.14 ± 0.01
P_3, midpoint pressure, mmHg	113 ± 5	117 ± 5	123 ± 3	117 ± 4
P_4				
Minimum SNA, %	28 ± 3	36 ± 9	41 ± 9	46 ± 11
Maximum gain, %/mmHg	5.0 ± 1.9	3.7 ± 0.7	2.5 ± 0.4	1.8 ± 0.4
		Peripheral arc		
R^2	0.67	0.68	0.48	0.43
Regression line	$y = 0.88x + 59.6$	$y = 0.54x + 61.7$*	$y = 0.57x + 66.7$†	$y = 0.35x + 46.3$*†
		Total baroreflex		
P_1, response range, mmHg	60 ± 8	61 ± 10	47 ± 5	30 ± 5†
P_2, slope coefficient, mmHg^{-1}	0.16 ± 0.02	0.18 ± 0.06	0.18 ± 0.02	0.14 ± 0.02
P_3, midpoint pressure, mmHg	112 ± 4	116 ± 7	122 ± 3	113 ± 4
P_4				
Minimum AP, mmHg	86 ± 7	80 ± 5	85 ± 7	58 ± 3*†
Maximum gain	2.3 ± 0.4	2.3 ± 0.4	2.0 ± 0.2	0.9 ± 0.1*†
		Equilibrium diagram		
Operating point AP, mmHg	113 ± 5	114 ± 5	116 ± 3	84 ± 5*†
Operating point SNA, %	60 ± 5	97 ± 7*	82 ± 8†	95 ± 4

Values are means ± SE; n, no. of rats. HUT, head-up tilt; SNA, sympathetic nerve activity. *$P < 0.05$, comparing HUT to prone in the same group. †$P < 0.05$, comparing VL to sham in the same position.

separately, and these two systems might be involved in a functional interaction. This putative interaction was quantitatively analyzed in the anesthetized sham and VL rats using an open-loop baroreflex analysis.

HUT shifted the neural arc to a higher SNA level and shifted the peripheral arc to a lower AP level in sham rats. Consequently, AP at the operating point was maintained by increased SNA. Using the same experimental setup, Kamiya et al. (19) first demonstrated the HUT-induced upward neural arc shift in rabbits, although the mechanism underlying this phenomenon remained unclear. In the present study, the HUT-induced upward shift of the neural arc was completely abolished in the VL rats, indicating that the vestibular system is responsible for this shift. In fact, a lateral and pitch-direction tilt or the linear acceleration stimulates the otolith organ and alters vestibular nucleus activity (3, 29), which might alter SNA through the vestibulo-sympathetic reflex (2, 11, 17, 23, 30, 32, 40). Projection to the nucleus tractus solitarius and then the rostral ventrolateral medulla may be responsible for this sympathoexcitation (4, 34, 45). Functional convergence from the vestibular and baroreceptor afferents to the same nuclei in the nucleus tractus solitarius and the rostral ventrolateral medulla further suggests that this is the central point of interaction between the vestibular system and the baroreflex (7, 45).

Postural change from prone to HUT induces a downward fluid shift and reduces the effective circulating blood volume, reducing venous return, cardiac output, and AP (43). The reduced circulating blood volume shifts the peripheral arc to a lower AP level (35). To minimize these effects, it is important to increase the venous tone and then reduce venous compliance (12). This might be achieved by a vestibular-mediated increase in SNA, which innervates the vein. The lower shift of the peripheral arc was smaller in the sham rats than in the VL rats, suggesting that lower body blood pooling in the sham rats was less than that in the VL rats. However, Yavorcik et al. (46) found no difference in lower limb blood pooling during HUT

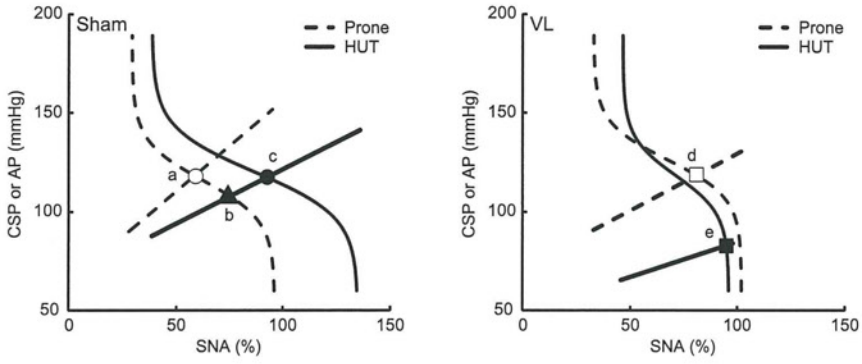

Fig. 6. Baroreflex equilibrium diagram constructed using the fitted logistic function for the neural arc and the regression line for the peripheral arc in vestibular-intact (sham) (*left*) and VL (*right*) rats. The intersection of the open circle (a) indicates the operating point of the prone position, and the solid circle (c) indicates the operating point of the HUT position in the sham rats. The intersection of the solid triangle (b) indicates the operating point without a HUT-induced neural arc shift in the sham rats. The intersection of the open square (d) shows the operating point of the prone position, and the solid square (e) shows the operating point of the HUT position in the VL rats.